

This is the accepted manuscript version of the contribution published as:

Ni, X., Dong, Z., Jiang, Y., Xie, W., Yao, H., **Chen, M.** (2022):
A subjective-objective integrated multi-objective decision-making method for reservoir operation featuring trade-offs among non-inferior solutions themselves
J. Hydrol. **613, Part A** , art. 128430

The publisher's version is available at:

<http://dx.doi.org/10.1016/j.jhydrol.2022.128430>

A subjective-objective integrated multi-objective decision-making method for reservoir operation featuring trade-offs among non-inferior solutions themselves

Xiaokuan Ni ^{1,2}, Zengchuan Dong ^{1*}, Yong Jiang ², Wei Xie ³, Hongyi Yao ⁴, Mufeng Chen ⁵

1 College of Hydrology and Water Resources, Hohai University, Nanjing, China

2 Department of Water Resources and Ecosystems, UNESCO-IHE Institute for Water Education, Delft, The Netherlands

3 Department of hydropower and water conservancy engineering, POWERCHINA Huadong Engineering Corporation Limited, Hangzhou, China

4 Department of Civil Engineering, The University of Hong Kong, Hong Kong, China

5 Department of Aquatic Ecosystem Analysis and Management, Helmholtz Centre for Environmental Research – UFZ, Magdeburg, Germany

* (Corresponding author) Zengchuan Dong, E-mail: zcdong@hhu.edu.cn

Highlights:

- A preference decision method (PDM) is developed to assist in making trade-offs.
- The PDM provides solid quantitative support for subjective preferences.
- The PDM draws on economic theories and has physical and mathematical connotations.
- The PDM is based on the Pareto set itself and can be extended into other areas.

Abstract: The key to formulating a multi-objective reservoir operation scheme is coordinating the high/low priorities and achieving balance among various targets accordingly in the decision-making process. However, the traditional decision-making methods are either completely subjective or neglect the decision-maker's preferences, making it essential to optimize these methods to address such unsatisfactory aspects. Therefore, through drawing on some universally acknowledged economic theories and studying the geometric relationships among the Pareto solutions to such multi-objective decision-making problems, the concepts of "replacement rate", "profit-loss sensitivity ratio", and "preference equilibrium degree" are introduced, deduced, and elaborated on in this paper. On the basis of them, the preference decision method (PDM), entrusted with strict mathematical and physical connotations, is constructed and derived in detail, especially for addressing the bi-objective and tri-objective scenarios. The PDM can quantify the complex internal feedback relationship among various targets, providing objective support for decision-makers in the subjective trade-offs of the interests of multiple subjects and achieving the unity of subjective and objective. Furthermore, the proposed method is applied to the Wujiang cascade reservoirs in China, through which the benefits of power generation, water supply and ecological protection are enabled to be considered simultaneously. The application shows that the PDM can effectively shrink the Pareto set, which greatly reduces the difficulty of decision-making, and the obtained results prove feasible and satisfactory. In addition, the PDM is based entirely on the Pareto set itself, making it simple to utilize, and can be extended into solving other multi-objective decision-making problems.

Keywords: Multi-objective decision-making, Trade-off, Preference, Reservoir operation, Utility, Gini coefficient

1 Introduction

A reservoir can change the natural runoff process through water storage and discharge to alleviate the uneven temporal distribution of water resources (Wang et al., 2016). With the growing population and awareness of environmental issues, the functional requirements for reservoirs have been continuously expanding, not only concerning the initial objective of power generation but also to those of water supply, ecological protection, flood control, shipping, and others (Bai et al., 2015; Yang et al., 2016; Liu et al., 2017; Cruz Courtois et al., 2021; C. Wu et al., 2022). However, irreconcilable conflicts among these goals do exist, leading to one goal often being achieved at the expense of others (Wang et al., 2020). Therefore, it is rather tricky and of concern to find a comprehensive, satisfactory scheme to achieve the best benefits of all objectives in the actual decision-making process of reservoir operation.

The key to formulating a feasible reservoir operation scheme is to cope with the relationships among various competitive or coordinated targets that are difficult to quantify, sort out the priorities and achieve balance among them, which essentially turns into a multi-objective decision-making problem (MODP) (Labadie, 2004; Ngo et al., 2007). Generally, for addressing MODPs, there are three available solving techniques: priori, progressive and posteriori (Coello Coello et al., 2002). The priori and progressive techniques can transform a multi-objective problem (MOP) into a single-objective one. Yet, with either of the two methods applied, abundant information is omitted, which theoretically could have been taken into consideration to some extent, and the decision-makers can hardly compare their final decisions with the other schemes to obtain a comparatively reliable support. While the posteriori technique has gained an edge over them in that through this technique, a more comprehensive decision-making scheme set can be obtained with relatively less interference by subjective factors and higher computational efficiency. Thus, it has been widely used in the current multi-objective operation of reservoir groups (Yang et al., 2020).

The posteriori techniques include two processes, multi-objective optimization (MOO) and multi-criteria decision-making (MCD) (Ridha et al., 2021). With the

development of multi-objective evolutionary algorithms, the "Pareto frontier" emerges, representing a set of non-dominated solutions regarding conflicts and incomparability among objectives (Cohon, 1978), and is considered the carrier and direct embodiment of multi-dimensional targets' interactive feedback relations. How to obtain the Pareto approximate of the optimization problem is something that the MOO process has been working on. In comparison, the MCD process requires selecting and ranking a group of available choices leveraging the obtained information (Garg and Kumar, 2018). During the process, a final choice will be made after a thorough review of the several indices of different implementable operation schemes, manifesting various benefit combinations of the objectives mentioned beforehand.

The Pareto sets carrying immense information gradually become the central processing target of MCD, with the posteriori technique introduced and utilized. According to real-time information, decision preferences and some other information, some specific evaluation methods or screening tools are to be used to sort and optimize the Pareto set and select one solution (Malekmohammadi et al., 2011). Such a solution represents a satisfactory scheme that meets the actual needs. One evaluation method commonly applied to such kinds of problems is the "simple additive weighting method" (maximum-minimum weighting method) (Saaty, 2003). Though intuitive, the method can be somewhat subjective when assigning weights to different objectives. In fact, it isn't easy to establish a generally satisfactory weighting method because the benefits of different objectives can vary greatly in importance in different situations. With the deepening of research, new evaluation methods and theories such as Analytic Hierarchy Process (AHP) (Li et al., 2020), Grey System (GS) (Li et al., 2015; Luo and Wang, 2012), Vague Set (VS) (Alhazaymeh and Hassan, 2015; Şahin and Liu, 2017), Set pair Analysis (SPA) (Garg and Kumar, 2018) and Fuzzy Decision Method (FDM) (Baghapour et al., 2020) have provided new ideas for addressing MCD.

Unfortunately, these decision-making methods are subjective or have no precise physical meaning. They fail to answer the critical question of how an increase or decrease in one benefit will lead to changes in other benefits, leaving the decision-makers in a "chaotic" state. In addition, formulating a qualified reservoir operation

scheme requires reasonably considering the decision makers' subjective preferences and providing them with enough objective information to assist them in clearly understanding the consequences and implications of their choice and preference. It is a great challenge to quantify the trade-offs among objectives of the cascade reservoir system (Smith et al., 2019), which is essential and critical for decision-makers and stakeholders to make more rational decisions on operation schemes.

Concerning dealing with the relationships of different objectives and making trade-offs, visual analysis is one of the most basic tools that vividly visualize the trade-offs among objectives in graphical form (Reed and Kollat, 2013). It can help identify key decision variables and guides the balanced regulation of multi-objective benefits (Kim et al., 2006). The visual analysis has been effectively applied in dealing with trade-off problems such as water allocation (Fu et al., 2013), reservoir operation (Hurford et al., 2014), and sewage treatment (Meng et al., 2016). Nevertheless, visual analysis usually fails to fully reveal the complex relationships among objectives or to assess their competitiveness objectively, which means that further research is needed to quantify the interactive feedback among objectives.

Some scholars have focused on the geometric properties of the distribution of Pareto solutions in the objective space. Some scholars have made some explorations on enhancing visual analysis. Tang et al. (2019) defined the Conflict Evaluation Index by projecting the Pareto frontier and measuring the distribution range of the projection to evaluate the intensity of competition quantitatively. Wu et al. (2020) derived the substitutive relationship between power generation and ecological protection by fitting the mathematical expression of the frontier. Wang et al. (2022) proposed two indicators, "Competitiveness Index" and "Competition Efficiency Index", to reconstruct the Pareto set between the two objectives to reduce the decision difficulty. Regarding the choice of specific solutions, the Technique for Order Preference by Similarity to an Ideal Solution (TOPSIS) (Tzeng and Huang, 2011) method is widely used. Further, based on the diminishing marginal substitution rate law, researchers believe that the "knee point" of the Pareto frontier has unique advantages. Li et al. (2021) find the tangent point to the Pareto front as the best compromise solution by constructing a linear spline utility

function of the Pareto front. X. Wu et al. (2022) defined the ratio of the slope of the line between the scattered points as a "Multi-objective Trade-off Index" to quantify the relationships among different objectives. However, these studies have done a lot of mathematical derivation, which is a meaningful attempt. Still, there is no strict physical connotation and cannot explain the practical significance of each step of the mathematical operation. In addition, through these methods, decision-makers can only be given a mathematically "optimal" choice without any opportunity to weigh trade-offs subjectively. More specifically, the research on quantitative trade-offs is still relatively preliminary, mostly limited to the analysis of two-dimensional relations, and there is a lack of effective analytical means for high-dimensional MCD.

In summary, the existing technology for the MCD in reservoir operation is still relatively rough. Usually, these decision methods are directly introduced into application situations and rarely combined with the interactive feedback relationships among the multiple objectives of the reservoir itself. As a result, it can be wholly subjective, or the decision-maker's preferences can not be considered.

However, these explorations are compelling and inspiring. By referring to the concepts of "price-performance ratio", "utility", and "Gini coefficient" in economics, this paper deduces the trade-offs among non-inferior schemes themselves in detail. It puts forward a novel practical ranking framework for MCD based on Pareto sets, namely the "preference degree decision-making method" (PDM). Compared to subjective methods represented by the AHP, the PDM is equipped with strict mathematical and physical connotations. Moreover, compared to objective methods based on "knee points", the PDM is capable of providing reliable support for decision-makers to make decisions according to their preferences and comprehensively realizing the integration of subjective and objective aspects.

The rest of this paper is organized as follows. Section 2 shows the detailed derivation process of the proposed PDM for the basic bi-objective situation and the extended tri-objective case regarding MCD. Section 3 takes the Wujiang River Basin in southwest China as a study case and establishes a cascade operation model for decision-making over three objectives: power generation, ecological protection, and

water supply. Section 4 applies the PDM to decision-making on optimal reservoir operation and discusses its advantages over existing methods. Section 5 concludes the paper.

2 Methodology

The trade-offs of multiple objectives in MCD are similar to some economic problems in the underlying logic. Based on this understanding, the PDM is proposed in this paper, and its analytical steps are summarized and shown in the following Figure 1. The corresponding mathematical derivation is carried out as below.

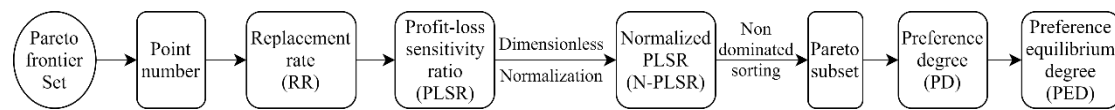


Figure 1 Methodology of preference degree decision-making method (PDM)

2.1 PDM for Bi-objective Optimization Problems

Assuming that $x_n (n=1,2,\dots,N)$ is one of the non-inferior solutions of a MOP with a population size of N , the Pareto solution set of the problem is $X = \{x_1, x_2, \dots, x_n, \dots, x_N\}$. The solutions to all actual problems, whether their original objective form is *min-max* or *min-min (max-max)*, can eventually be transformed into a *min-min (max-max)* form by adding a positive or negative sign to the objective function. Based on this, this paper's subsequent derivation of the quantification process for the Pareto frontier is carried out in the objective space of the *min-min* form.

In real life, when people buy items, they often consider how much more services can be obtained by spending an additional amount of money to measure the affordability of items which is the "price-performance ratio" (Schindele et al., 2020). Comparably, in terms of a bi-objective optimization problem, any non-inferior solution, x_n , corresponds to an objective function value, (f_1^n, f_2^n) , of two dimensions. To quantify the extent to which a change in the value of one objective function causes a change in another objective, with reference to the "price-performance ratio", a novel concept, "replacement rate", was put forward in this paper denoted as r . And the following definitions apply.

Definition 1: replacement rate (RR). Replacement rate, r_1 (r_2), is the absolute average tangent value of the intersection angles, θ_1 (θ_2), between the vectors (formed by any point on the Pareto front and both its two adjacent points separately) and their corresponding f_1 -axis (f_2 -axis) components. In particular, for either of the two endpoints of the Pareto front, the vector is formed by the point itself and the nearest adjacent point, and r_1 (r_2) equals the absolute tangent value of the intersection angle between the vector and its corresponding f_1 -axis (f_2 -axis) component.

First, all non-inferior solutions are numbered with i ($i = 1, 2, \dots, N$) according to the order of values of the objective function, f_1 , sorted from small to large. All of the functions corresponding to the i -th solution are numbered with i as well. And then the RR of the two objective functions corresponding to each solution, numbered with i , on the Pareto frontier is:

$$r_1^i = \overline{\tan \theta_1^i} = \begin{cases} \left| \frac{f_2^2 - f_2^1}{f_1^2 - f_1^1} \right| & i = 1 \\ \frac{1}{2} \left(\left| \frac{f_2^i - f_2^{i-1}}{f_1^i - f_1^{i-1}} \right| + \left| \frac{f_2^{i+1} - f_2^i}{f_1^{i+1} - f_1^i} \right| \right) & i = 2, 3, \dots, N-1 \\ \left| \frac{f_2^N - f_2^{N-1}}{f_1^N - f_1^{N-1}} \right| & i = N \end{cases} \quad (1)$$

$$r_2^i = \overline{\tan \theta_2^i} = \begin{cases} \left| \frac{f_1^2 - f_1^1}{f_2^2 - f_2^1} \right| & i = 1 \\ \frac{1}{2} \left(\left| \frac{f_1^i - f_1^{i-1}}{f_2^i - f_2^{i-1}} \right| + \left| \frac{f_1^{i+1} - f_1^i}{f_2^{i+1} - f_2^i} \right| \right) & i = 2, 3, \dots, N-1 \\ \left| \frac{f_1^N - f_1^{N-1}}{f_2^N - f_2^{N-1}} \right| & i = N \end{cases} \quad (2)$$

where, i is the number assigned to the non-inferior solutions based on the ascending order of values of the objective function f_1 ; N is the total number of non-inferior solutions; r_1^i (r_2^i) is the RR of f_2 relative to f_1 (f_1 relative to f_2) at the i -th non-inferior solution, which, hereinafter, is described as the RR of f_1 (f_2); θ_1^i (θ_2^i) is the intersection angle between the vectors (formed by the i -th non-inferior solution point and both adjacent points separately) and the f_1 -axis (f_2 -axis) components; f_1^i , f_2^i are

respectively the values of the two objective functions corresponding to the i -th non-inferior solution.

Taking the Pareto frontier of the bi-objective optimization benchmark test problem ZDT2 as an example, the geometric expression of the RR concept is shown in Figure 2 below.

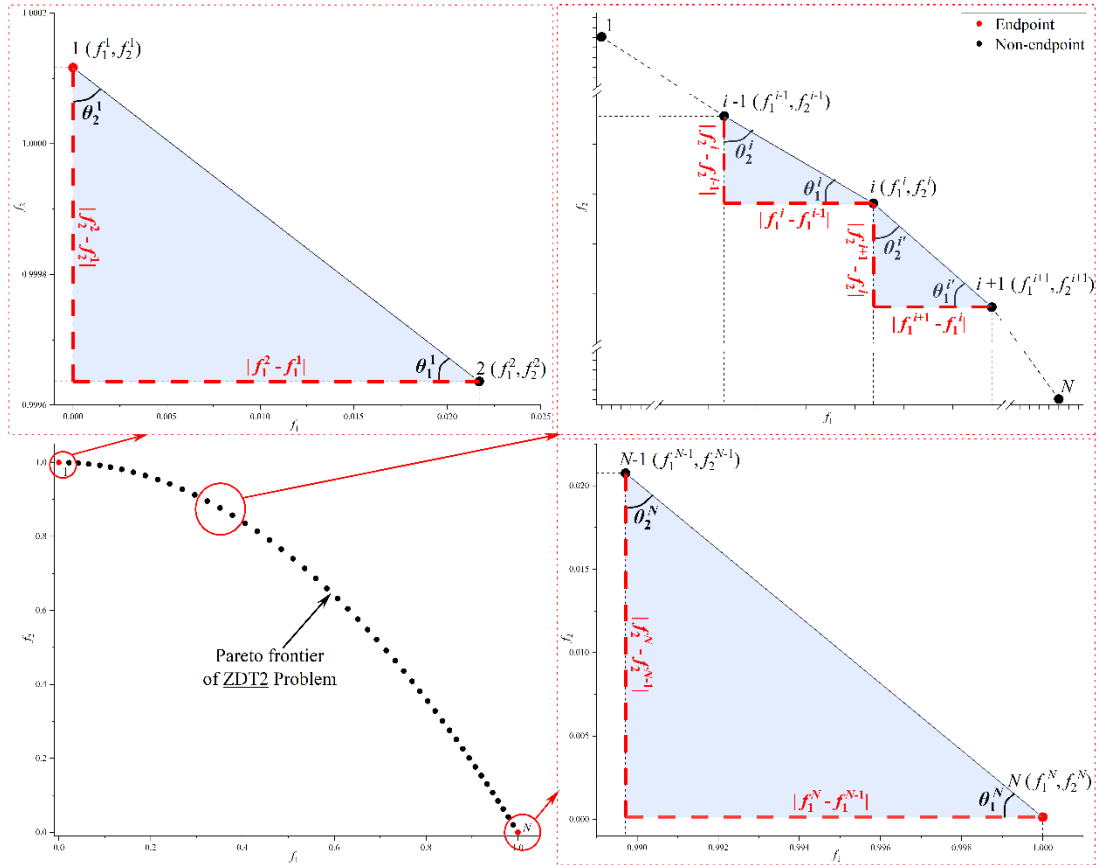


Figure 2 Geometric expression of replacement rate (RR) in bi-objective optimization problems

Actually, even if the absolute change of one objective function remains the same when the other objective function values change by one unit, the relative impact considerably varies depending on the place of the objective function values where such change occurs. That's why decision-makers often consider the relative influence degree rather than the absolute value change in engineering practice, which is similar to the law of diminishing marginal utility (Brewer and Venaik, 2010) in economics, manifesting that when consumers consume a certain commodity incrementally, the total utility may still increase, whereas the unit utility of the goods is gradually decreasing. Therefore, to meet the needs of examining the relative influence degree in multi-

objective decision-making, the concept "profit-loss sensitivity ratio" was proposed and defined below, denoted as δ , with the concept of "unit utility" in economics used for reference.

Definition 2: profit-loss sensitivity ratio (PLSR). Profit-loss sensitivity ratio is the ratio of the RR of one axis component (f_1 or f_2) to the corresponding objective function value for a non-inferior solution on the Pareto frontier. The formula is as follows.

$$\delta_1^i = \frac{r_1^i}{f_1^i} \quad (f_1^i \neq 0) \quad i = 1, 2, \dots, N \quad (3)$$

$$\delta_2^i = \frac{r_2^i}{f_2^i} \quad (f_2^i \neq 0) \quad i = 1, 2, \dots, N \quad (4)$$

where, δ_1^i and δ_2^i are, respectively, the PLSR of f_1 and f_2 at the i -th non-inferior solution, which represents the sensitivity of the RR to the change of the objective function value.

Considering the different units and orders of magnitude of each objective in the actual MOPs, the PLSR is made dimensionless through data normalization as follows.

$$\varepsilon_1^i = \frac{\delta_1^i}{\sum_{i=1}^N \delta_1^i} \quad i = 1, 2, \dots, N \quad (5)$$

$$\varepsilon_2^i = \frac{\delta_2^i}{\sum_{i=1}^N \delta_2^i} \quad i = 1, 2, \dots, N \quad (6)$$

where, ε_1^i and ε_2^i are, respectively, the normalized PLSR (N-PLSR) of f_1 and f_2 at the i -th non-inferior solution.

At this point, with the concepts of "price-performance ratio" and "unit utility" in economics utilized for reference, the degree of gains or losses caused by each non-inferior solution of MOPs can be quantitatively compared through the RR and PLSR. However, there are too many individuals in the Pareto set, making it unrealistic to compare all of them in actual decision-making. Therefore, optimizing the decision-making process and improving the simplicity of trade-offs is necessary.

The concept of non-dominated sorting is used for reference to simplify the scope of decision-making. The dominance relationship of either set of N-PLSRs, $\{\varepsilon_1\}$ and $\{\varepsilon_2\}$, is compared, a non-inferior solution subset is acquired by secondary screening, and finally, the solution individuals, most sensitive to profit and loss, are obtained and included in the decision support set:

$$X^* = \{x^u \in X \mid \exists x^v \in X, \exists \varepsilon_1^v > \varepsilon_1^u \ \& \ \varepsilon_2^v > \varepsilon_2^u\} \quad (7)$$

where, X^* is the decision support set, that is, the subset of non-inferior solutions after screening; X is the original non-inferior solution set; x^u and x^v represent different non-inferior solution individuals with different numbers.

According to the physical meaning of the PLSR, for an individual solution, the obtained profit and loss percentage will change faster with a more considerable relative weight of PLSR for one target. Thus the decision-makers are prone to select and optimize this target to achieve greater benefits. Based on such understanding, on the basis of the N-PLSR, a concept, "preference degree", is proposed in this paper, denoted as ω , the value range of which is (0, 1).

Definition 3: preference degree (PD). Preference degree is the relative weight of the N-PLSR for the two axis components of each solution in the decision support set. The calculation formula is as follows.

$$\omega_1^m = \frac{\varepsilon_1^m}{\varepsilon_1^m + \varepsilon_2^m} \quad m = 1, 2, \dots, M \quad (8)$$

$$\omega_2^m = \frac{\varepsilon_2^m}{\varepsilon_1^m + \varepsilon_2^m} \quad m = 1, 2, \dots, M \quad (9)$$

where, M is the scale of decision support set X^* ; m is the number assigned to the element in the decision support set based on the order of values of the objective function, f_1 , arranged in ascending order; ω_1^m and ω_2^m are the PDs of m -th non-inferior solution towards the objective function f_1 and f_2 , respectively. There is $\omega_1^m + \omega_2^m = 1$.

The PD (ω_1^m, ω_2^m) essentially reflects the extent to which the decision-makers prefer to optimize one specific objective at each individual solution on the Pareto

frontier. Thus it can be used as the preference weight of different optimization objectives.

Notwithstanding, in actual decision-making, comparing different combinations of preference degrees one by one is rather time-consuming and labour-intensive, leading to an index needed to unify the preference degrees towards different goals. Based on the Lorenz curve, the Gini coefficient (Ceriani and Verme, 2012) is often used to express the degree of equality of income distribution in economics. To be more specific, assuming that the enclosed area between the actual income distribution curve and the absolute equality curve is A, and the area at the lower right of the actual income distribution curve is B, the quotient of A divided by (A + B) is defined as "Gini coefficient". Enlightened by it, the equilibrium degree of objective preference can be measured by calculating the proportion of the envelope area to unify the preference degrees towards different objectives. Therefore, referring to the concept of "Gini coefficient" in economics, the concept of "preference equilibrium degree" was proposed in this paper, denoted as E , with its value range $[0, 1]$.

Definition 4: preference area (PA). The preference area is the rectangular area formed by a PD's two-axis components (as two lateral edges) at a non-inferior solution. In particular, if the two axis components of the preference degree are equal, the area turns out to be the largest, called the balanced preference area (BPA). The value range of PA is $[0, 0.25]$. And the geometric expression of the PA is shown in Figure 3.

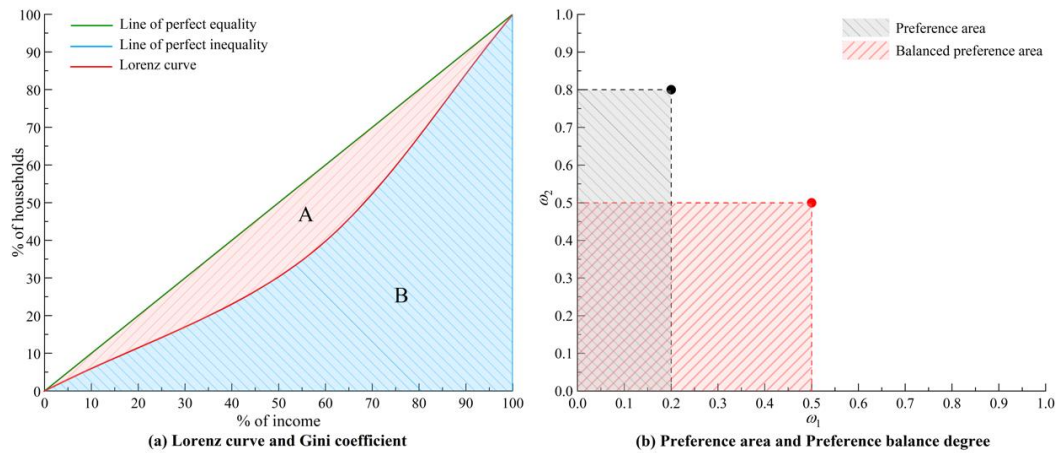


Figure 3 Geometric expression of Lorenz curve and preference area (PA)

Definition 5: preference equilibrium degree (PED). The preference equilibrium

degree is the quotient of actual PA divided by BPA, calculated as follows:

$$E^m = \frac{\omega_1^m \cdot \omega_2^m}{1/4} \quad (10)$$

Where E^m represents the PED at m -th non-inferior solution, with its value range $[0, 1]$, the higher the value, the more the bias towards the two objectives converges.

The PED at each non-inferior solution, combined with the specific PD, can be used for reference to provide a feasible and effective solution for decision-making.

The economic concepts involved in the proposed method (PDM) and their mapping are shown in Table 1 below.

Table 1 Economics concepts reference in PDM and their mapping relationships

Economics concepts	Mapping connotation	Mapping concepts
Price-performance ratio	Influence degree	Replacement rate (RR)
Unit utility	Relative influence degree	Profit-loss sensitivity ratio (PLSR)
Gini coefficient	Equilibrium degree	Preference equilibrium degree (PED)

2.2 PDM for Tri-objective Optimization Problems

Based on the research on the bi-objective optimization problems, taking the *min-min-min* problem as an example, the PDM was further developed and expanded in this paper to address the tri-objective optimization decision-making problems.

Following the idea of coping with two-objective optimization problems, the individuals are numbered in the non-inferior solution set X of the tri-objective optimization problems. Whereas, compared with the bi-objective optimization problems, the spatial distribution of the Pareto frontier of the tri-objective optimization problems is way more complex.

As for the bi-objective problems, a specific value of the objective function f_1 corresponds to a unique value of f_2 , meaning that there will be a unique solution individual. However, in the tri-objective problems, a specific value of the objective function f_1 may correspond to multiple solution individuals, for which the numbering method needs to be improved. The new numbering system is implemented according to the order of distance values, L_n , arranged in ascending order between the non-inferior

solution individuals $x_n(f_1^n, f_2^n, f_3^n)$ and the origin of spatial coordinates $O(0,0,0)$.

$$L_n = \sqrt{(f_1^n)^2 + (f_2^n)^2 + (f_3^n)^2} \quad (11)$$

where, L_n is the spatial Euclidean distance between the non-inferior solution individual and the origin.

The RR is also used for tri-objective optimization problems to quantitatively investigate the change degree of the other two objectives caused by the value change of one objective function. In calculating the RR, it is a precondition to discern one or two points adjacent to a specific point on the Pareto front based on the new numbering system. However, compared with the bi-objective problems, where the adjacent points can be found simply by discerning the number assigned to the solution individuals, the process is more complex for the tri-objective optimization problems. First, the spatial Euclidean distance between the point x_i and the other points on the Pareto front is calculated with:

$$L_{ii'} = \sqrt{\sum_{o=1}^3 (f_o^i - f_o^{i'})^2} \quad (12)$$

where, $L_{ii'}$ is the Euclidean distance between two solution individuals i and i' , o is the number of objective functions, $o = 1,2,3$.

The two points with the shortest spatial Euclidean distance from x_i are selected, denoted as the nearest point x_j and the second-nearest point x_k . Then, it is judged whether the sequent connection of x_j , x_i and x_k is strictly monotonically increasing/decreasing or not, i.e. whether it meets the following requirements:

$$\begin{cases} f_1^j < f_1^i < f_1^k \square f_1^j > f_1^i > f_1^k \\ f_2^j < f_2^i < f_2^k \square f_2^j > f_2^i > f_2^k \\ f_3^j < f_3^i < f_3^k \square f_3^j > f_3^i > f_3^k \end{cases} \quad (13)$$

If satisfied, x_i is called an internal point, otherwise, an external point. In particular, when an external point x_i and its nearest point x_j meet the requirement of $(f_1^i = f_1^j) \square (f_2^i = f_2^j) \square (f_3^i = f_3^j)$, the external point x_i actually becomes a two-dimensional (2D) point. Assuming that X_1 is the set composed of all internal points, X_2

of all external points and X_3 of all 2D points, it is evident that the relationship between the three sets is as follows:

$$\begin{cases} X_1 \cup X_2 = X \\ X_1 \cap X_2 = \emptyset \\ X_3 \subseteq X_2 \end{cases} \quad (14)$$

Referring to the definition of the RR in the bi-objective optimization problems, the calculation rule of the tri-objective RR is formulated as follows. As for an internal point, it is the average tangent value of the intersection angles between the vectors (composed of the specific point and its nearest point/second-nearest point separately) and the corresponding axis component, respectively. For an external point, it is the tangent value of the intersection angle formed by the vector (composed of the point and its nearest point) and the corresponding axis component. In particular, for 2D points, the RR of the objective dimensions with equal values is 0.

$$r_o^i = \begin{cases} (\tan \theta_o^{ij} + \tan \theta_o^{ik})/2 & x_i \in X_1 \\ \tan \theta_o^{ij} & (f_o^i \neq f_o^j) \quad x_i \in X_2 \\ 0 & (f_o^i = f_o^j) \quad x_i \in X_3 \end{cases} \quad (o=1,2,3) \quad (15)$$

$$\tan \theta_o^{ij} = \frac{\sqrt{\sum_{a=1, a \neq o}^3 (f_o^i - f_o^j)^2}}{|f_o^i - f_o^j|} \quad (16)$$

where, i is the number of a non-inferior solution; r_o^i is the RR of the o -th objective relative to the other two objectives at the i -th non-inferior solution; θ_o^i is the angle between the vector (formed by the i -th non-inferior solution and its nearest point/second-nearest point separately) and its o -th axis components; f_o^i is the value of the o -th objective function at the i -th non-inferior solution.

Taking the Pareto frontier of the tri-objective optimization benchmark test problem DTLZ2 as an example, the geometric expression of the concept of tri-objective RR is shown in Figure 4.

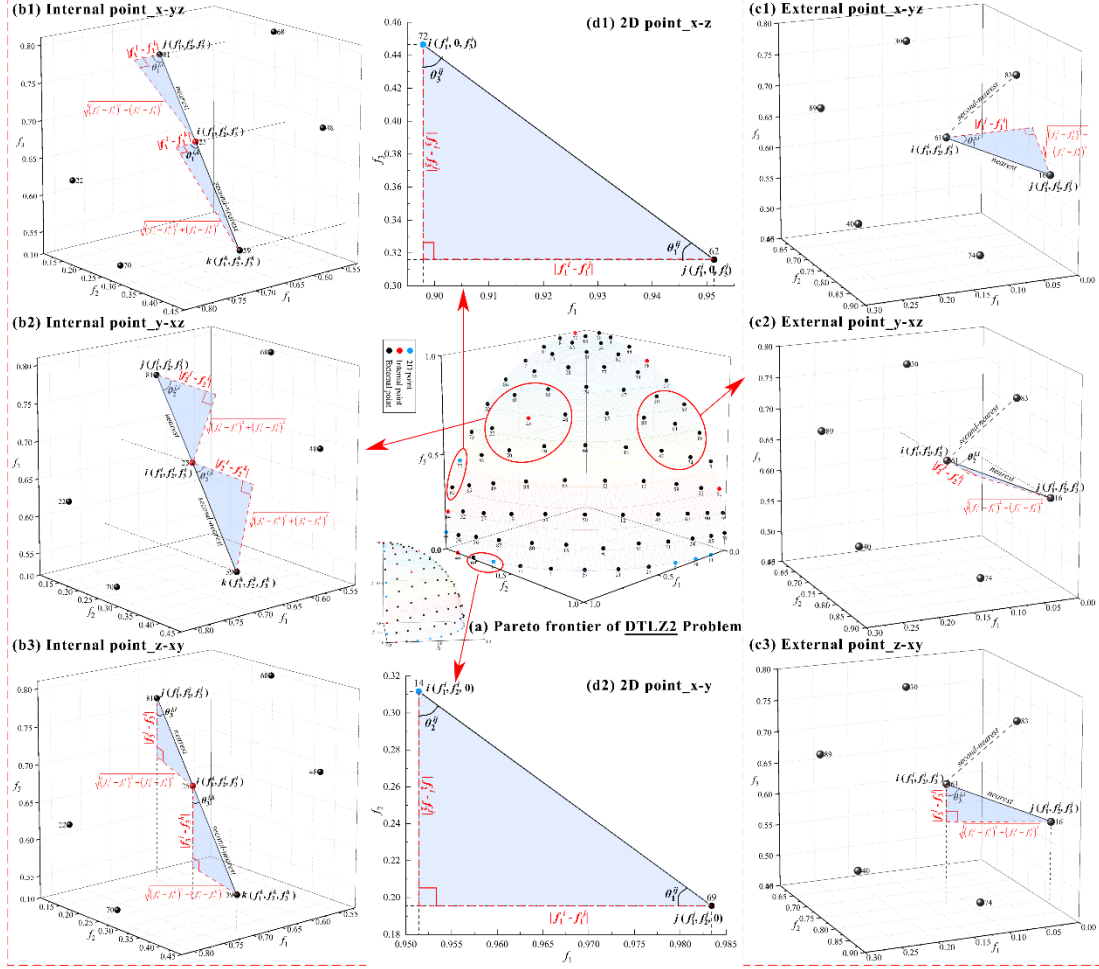


Figure 4 Geometric expression of RR in tri-objective optimization problems

Furthermore, the PLSR for the tri-objective optimization problems are calculated with:

$$\delta_o^i = \frac{r_o^i}{f_o^i} \quad (f_o^i \neq 0) \quad x_i \in X \quad (o=1,2,3) \quad (17)$$

$$\varepsilon_o^i = \frac{\delta_o^i}{\sum_{i=1}^N \delta_o^i} \quad (o=1,2,3) \quad (18)$$

where, δ_o^i is the PLSR of the o -th objective function at the i -th non-inferior solution, and ε_o^i is the N-PLSR.

According to the non-dominated sorting principle, the decision support set via secondary screening is:

$$X^* = \{x^u \in X \mid \text{no } x^v \in X, \exists \varepsilon_o^v > \varepsilon_o^u \quad (o=1,2,3)\} \quad (19)$$

And the PD of each solution individual in the decision support set is:

$$\omega_o^m = \frac{\varepsilon_o^m}{\sum_{o=1}^3 \varepsilon_o^m} \quad m = 1, 2, \dots, M \quad (o = 1, 2, 3) \quad (20)$$

Where, M is the scale of decision support set X^* ; m is the number assigned to an element in the decision support set based on the order of values arranged from small to large of its spatial Euclidean distance from the origin; ω_o^m is the PD of the m -th non-inferior solution towards the o -th objective. And there is $\sum_{o=1}^3 \omega_o^m = 1$.

In the bi-objective optimization decision-making problems, referring to the concept and calculation method of the Gini coefficient, the ideas of PA and PED are proposed and utilized in this paper to unify the different PDs of the two objectives. While to unify the PDs for the tri-objective optimization problems, it is necessary to expand the planar idea of PA to a spatial one, i.e. preference volume.

Definition 6: preference volume (PV). Preference volume is the cuboid volume formed by a PD's three-axis components (as three adjacent edges) at a non-inferior solution. In particular, if the three-axis components of the preference degree are equal, the volume turns out to be the largest, called the balanced preference volume (BPV). The value range of PV is $[0, 1/27]$. And the geometric expression of the PV is shown in Figure 5.

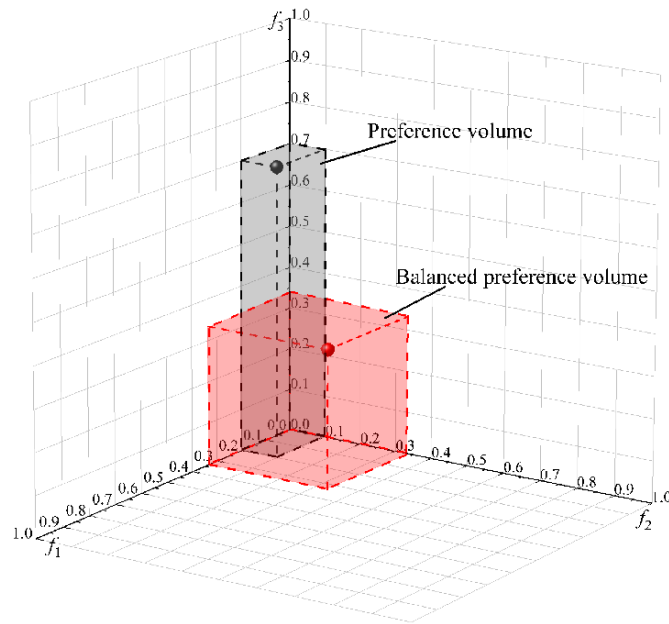


Figure 5 Geometric expression of preference volume (PV)

Furthermore, as for the tri-objective optimization problems, the PED is the quotient of the actual PV and the BPV, the formula of which is as follows.

$$E^m = \frac{\prod_{o=1}^3 \omega_o^m}{1/27} \quad (21)$$

where, E^m is the PED of the m -th non-inferior solution, also its value range is $[0, 1]$, and the higher the value, the more the bias towards the three objectives converges.

The PDM proposed in this paper, respectively for the bi-objective and tri-objective optimization problems, are summarized and compared, as shown in Table 2 below:

Table 2 Comparison of the PDM for bi-objective and tri-objective optimization problems

Critical nodes	Bi-objective	Tri-objective	Core idea
Non-inferior solution numbering	Ascending order of values of the objective function f_1	Ascending order of the distance between individuals and the spatial origin	Sort to facilitate positioning
Replacement rate (RR)	The average tangent value of the intersection angles between the vectors and the corresponding axis		Absolute degree of change
Point category	Endpoint Non-endpoint	Internal point External point (2D point)	Special cases separated and discussed according to geometric characteristics
Profit-loss sensitivity ratio (PLSR)	$\frac{\text{RR value of one axis}}{\text{Corresponding objective value}}$		The relative degree of change
Nondimensionalization	Normalization		Enhance comparability of PLSR
Non-inferior solution subset	Non-dominating sorting of N-PLSR		Narrow decision-making scope
Preference degree (PD)	$\frac{\text{Specific objective's N-PLSR}}{\text{Sum of all objectives' N-PLSR}}$		Preference quantization
Preference equilibrium degree (PED)	Preference area (PA)	Preference volume (PV)	Equilibrium degree

3 Case study

To demonstrate the effectiveness of the proposed PDM, the study applies the method to the operational decision-making of the cascade reservoirs on the Wujiang River to examine trade-offs among power generation, water supply and ecological protection.

3.1 The study area

The Wujiang River basin is located at 104°18' ~ 109°22'E and 26°07' ~ 30°22' N, with a total area of 87920 km². The river, with its mainstream length of 1,037 km, is the largest tributary on the south bank of the upper Yangtze River and a representative river in southwest China. The Wujiang River basin has a natural drop of 2124 m and a channel gradient of 0.205%, rich in hydropower resources. Since the 1970s, China has carried out large-scale hydropower development in the Wujiang River basin and planned a 12-level development scheme in the mainstream. Except for the Baima navigation and hydropower project at the most downstream, all the planned hydraulic engineering projects have been completed. The geographical location and the water system distribution of the Wujiang River Basin are shown in Figure 6(a).

Out of the 12 reservoirs on the mainstream of the Wujiang River, five have the above-seasonal regulation capacity, and for the rest, the capacity is daily. For the runoff regulation, the reservoirs with above-seasonal capacity are comparatively worthy of investigation. The basic information about these five reservoirs is shown in Table 3. Their generalized topological relationships with rivers and important hydrological stations are shown in figure 6(b).

Table 3 Parameters of main reservoirs in the mainstream of the Wujiang River

Reservoir	Regulation capacity	Water level (m)			Beneficial capacity (×10 ⁸ m ³)	Installed capacity (MW)
		Dead	Normal	Flood control ¹		
Hongjiadu	over-year	1076	1140	1138	33.61	600
Dongfeng	seasonal	936	970	970	4.91	970
Wujiangdu	seasonal	720	760	760	13.6	1250
Goupitan	over-year	590	630	626.24/628.12	29.02	3000
Pengshui	annual	278	293	287	5.18	1750

¹: The flood season in the Wujiang River Basin is from June to August every year.

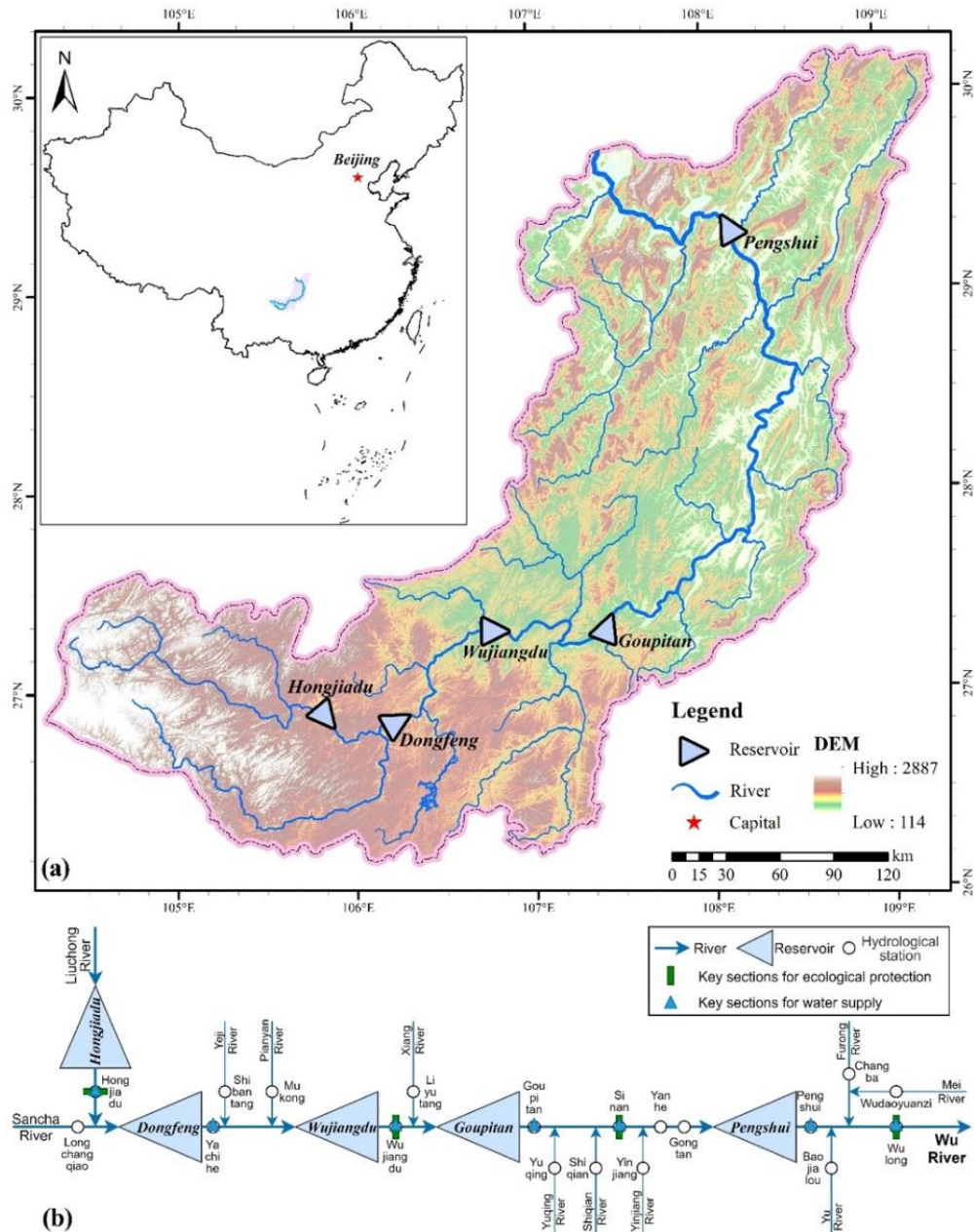


Figure 6 The map of the Wujiang River Basin (a) and generalized topological map of the cascade reservoirs group (b)

According to the document "*Water Distribution Plan of Wujiang River Basin*" issued by the Ministry of Water Resources of PRC, the key monitoring sections and requirements for water supply of Wujiang River Basin are articulated. Wei and Dong (2021) proposed four key sections about the ecological protection of the Wujiang River and established the minimum flow requirements for maintaining a healthy ecological condition. These key sections are also marked in Figure 6(b).

3.2 Multi-objective operation model of reservoir group

The complex demand for power generation, water supply and river ecological protection of the Wujiang River Basin can be abstracted into the following mathematical model, composed of three objective functions and five constraints related to reservoir operation.

3.2.1 Objective functions

(1) Energy target, the maximum total power generation (PG) of the cascade reservoirs is defined by:

$$f_1 = \max E = \max \left\{ \sum_{i=1}^I \sum_{t=1}^T (N_{i,t} \times \Delta t) \right\} \quad (22)$$

$$N_{i,t} = k_i q_{i,t} H_{i,t} \quad (23)$$

where, E (kW·h) is the total PG of the cascade reservoirs. I and T are the total number of cascade reservoirs and the total period length, respectively. $N_{i,t}$ (kW) is the output of the i -th reservoir during the t -th period, $q_{i,t}$ (m³/s) and $H_{i,t}$ (m) are the corresponding discharge and water head, respectively. k_i is the output coefficient of the i -th reservoir, and Δt (h) is the length of a specific interval.

(2) Water supply target, the maximum water supply guarantee rate (WSGR) is:

$$f_2 = \max G = \max \left\{ \left(\sum_{m=1}^M \sum_{t=1}^T G_{m,t} \right) / MT \right\} \quad (24)$$

$$G_{m,t} = \begin{cases} \frac{q_{m,t}}{D_{m,t}} & (q_{m,t} < D_{m,t}) \\ 1 & (q_{m,t} \geq D_{m,t}) \end{cases} \quad (25)$$

where, G is the total WSGR of the cascade reservoirs, and M is the total number of key sections for water supply. $G_{m,t}$ is the WSGR of the m -th section during the t -th period, and $D_{m,t}$ (m³/s) is the corresponding water demand flow requirement, designated by the "Water Distribution Plan of Wujiang River Basin" mentioned above.

(3) Ecological protection target, the maximum ecological satisfaction degree (ESD) is:

$$f_3 = \max S = \max \left\{ \left(\sum_{n=1}^N \sum_{t=1}^T S_{n,t} \right) / NT \right\} \quad (26)$$

$$S_{n,t} = \begin{cases} \frac{q_{n,t}}{Eco_{n,t}} & (q_{n,t} < Eco_{n,t}) \\ 1 & (q_{n,t} \geq Eco_{n,t}) \end{cases} \quad (27)$$

where, S is the total ESD of the cascade reservoirs, and N is the total number of key sections for ecological protection. $S_{n,t}$ is the ESD of the n -th section during the t -th period, and $Eco_{n,t}$ (m^3/s) is the corresponding optimal ecological flow, which refers to the achievements of Wei and Dong (2021).

3.2.2 Constraint conditions

(1) Water balance constraint

$$V_{i,t} - V_{i,t-1} = (Q_{i,t} - q_{i,t} - E_{i,t}) \Delta t \quad (28)$$

where, $V_{i,t}$, $V_{i,t-1}$ (m^3) are the storage capacity of the i -th reservoir at the end and the beginning of the t -th period, respectively. $Q_{i,t}$, $q_{i,t}$ and $E_{i,t}$ (m^3/s) are the average inflow, discharge, and loss of the i -th reservoir during the t -th period, respectively.

(2) Water-level constraint

$$Z_{i,t,\min} \leq Z_{i,t} \leq Z_{i,t,\max} \quad (29)$$

where, $Z_{i,t}$, $Z_{i,t,\min}$ and $Z_{i,t,\max}$ (m) are the real-time, lower limit, and upper limit water level of the i -th reservoir at the end of the t -th period, respectively.

(3) Discharge constraint

$$q_{i,t,\min} \leq q_{i,t} \leq q_{i,t,\max} \quad (30)$$

where, $q_{i,t,\min}$ and $q_{i,t,\max}$ (m^3/s) are the minimum and maximum discharge of the i -th reservoir during the t -th period, respectively, generally as a function of the corresponding reservoir water level.

(4) Output constraint

$$N_{i,t} \leq N_{i,t,\max} \quad (31)$$

where, $N_{i,t,\max}$ (kW) is the maximum output of the i -th reservoir during the t -th period, which is equivalent to the installed capacity of the reservoir.

(5) Discharge variation amplitude constraint

$$|q_{i,t} - q_{i,t-1}| \leq \Delta q_i \quad (32)$$

where, Δq_i (m^3/s) is the maximum discharge variation amplitude of the i -th reservoir, which aims to control the discharge, making it as stable as possible.

3.3 Datasets

This study extracted the daily runoff data of key hydrological stations in the Wujiang River Basin from the past 64 years (1956 ~ 2019) from the Hydrological Yearbook of the People's Republic of China. The study also reviewed the reliability, consistency and representativeness of the data.

The flow of three stations, respectively, Wujiangdu (upstream/midstream boundary section), Sinan (midstream / downstream boundary section) and Wulong (basin outlet section), were arranged by the P-III distribution (Zhang et al., 2018; Lei et al., 2019; Raynal Villaseñor, 2021). The flow values corresponding to the frequencies of 25%, 50% and 75% on the P-III curve are taken as the design values in wet, normal and dry years, respectively. Based on the flow situation of the upper, middle and lower reaches, three years, 1960, 1979 and 1976, in which the measured values are similar to the design values, were selected as typical years to represent the conditions of dry, normal and wet situations. The detailed parameters of reservoirs were obtained from the management departments.

4. Results and Discussion

The simulation of the multi-objective operation model in Section 3.2 was carried out using the measured flow data of three typical years as input, the discharge flows from individual reservoirs as the decision variable, with a 10-day operation scale. The solutions were dealt with through the improved VA-NSGA-III algorithm (Ni et al., 2019) to obtain the non-inferior ones in dry, normal and wet years.

4.1 Visual analysis

Drawing the non-inferior solution points of the three objective functions in the three-dimensional space. The Pareto frontiers of the MOP of Wujiang cascade reservoirs in typical dry, normal and wet years are shown in Figures 7-9 as below.

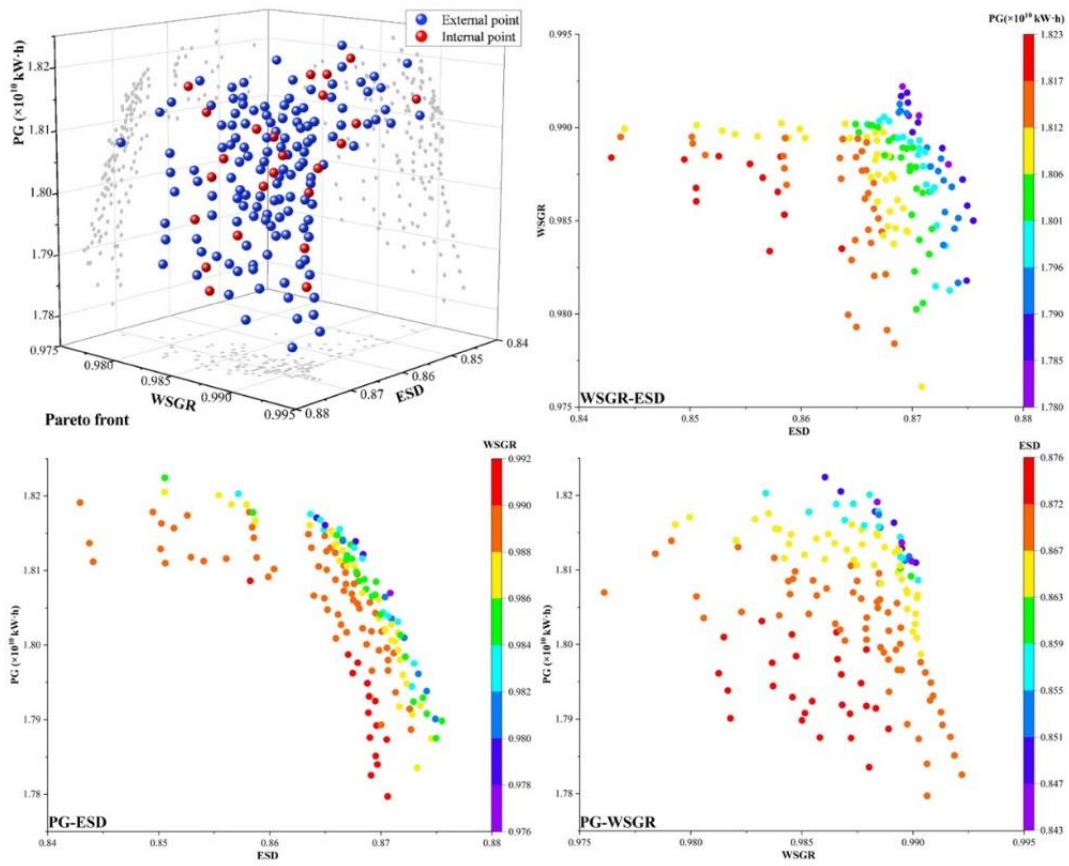


Figure 7 The Pareto frontier and its 2D projection in a typical dry year

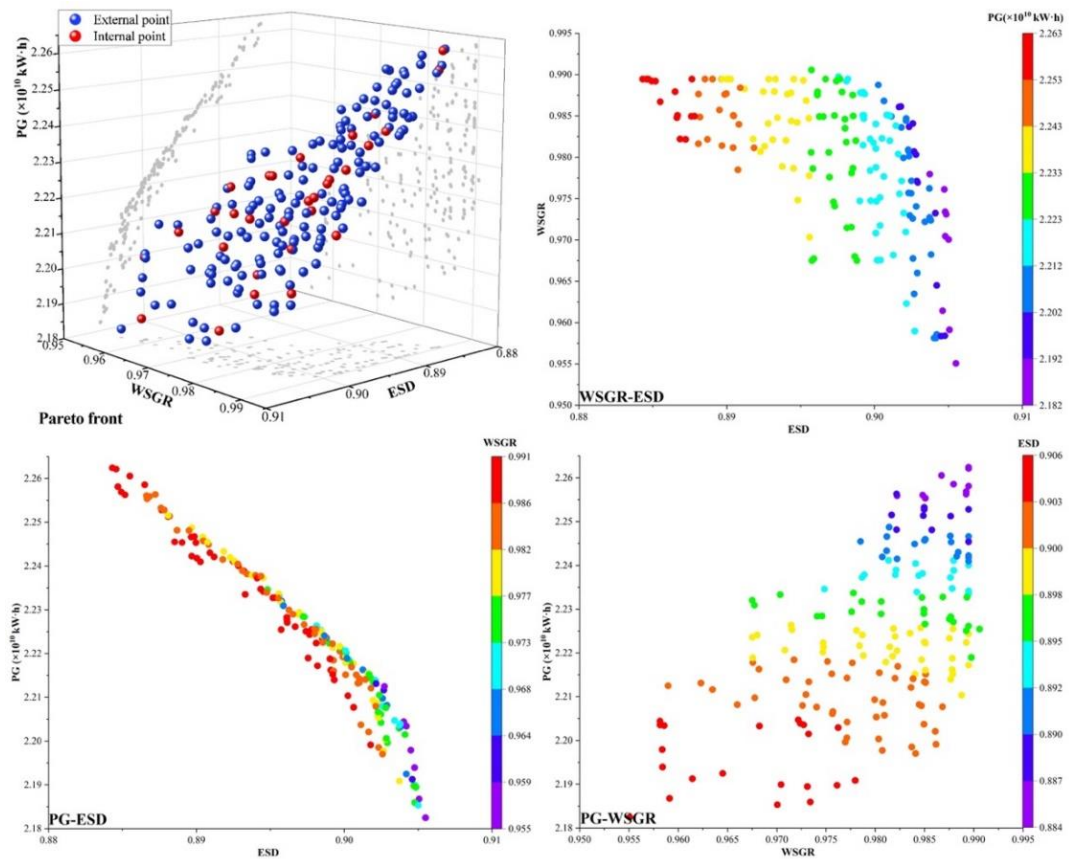


Figure 8 The Pareto frontier and its 2D projection in a typical normal year

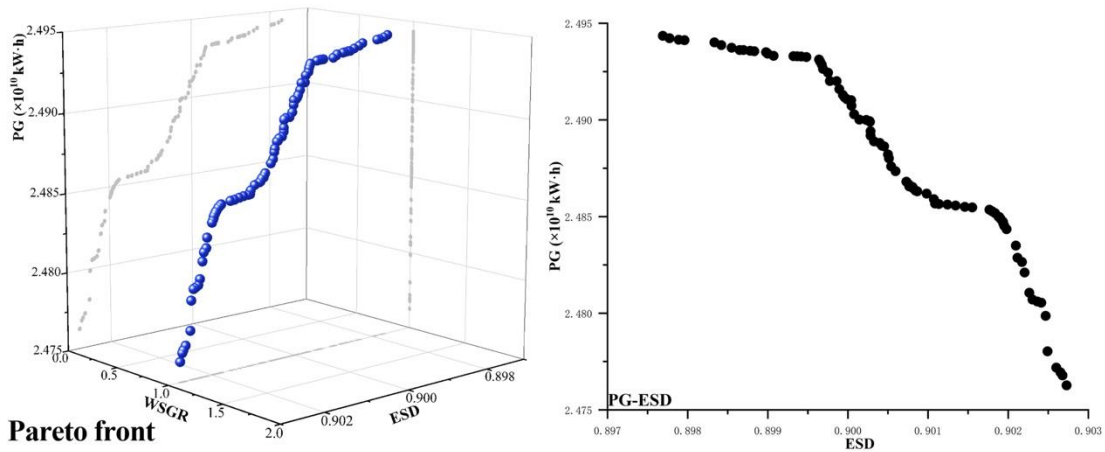


Figure 9 The Pareto frontier and its 2D projection in a typical wet year

In terms of the interrelationship of the various objectives, obviously, there is an intense competition between the two objectives of PG vs ESD. In contrast, the competitions between PG vs WSGR and WSGR vs ESD, although also observed, are significantly weaker.

In addition, looking more specifically at the benefit values for each objective, as shown in Figure 10, they played out differently under different hydrological conditions. All three targets can be better optimized when the inflow is abundant, of which the improvement of PG is the most obvious. In particular, the water supply target can be fully met in the wet year. From this, it can be inferred that inflow's positive role can be further exploited and augmented to the ecological benefit in a wet year and the water supply benefit in a normal year by reliably weighing.

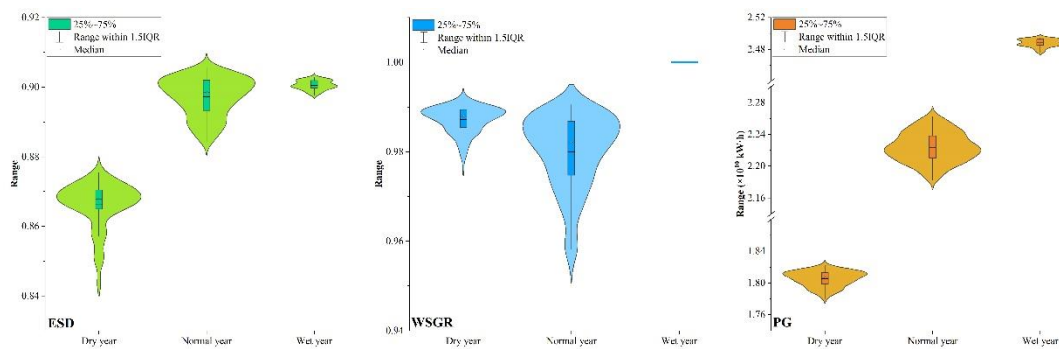


Figure 10 Distribution range of each target objective values in different typical years

Through visual analysis, it can be clearly understood that coordinating the three objectives of power generation, water supply, and ecological protection for the Wujiang cascade reservoirs effectively involves a trade-off between PG and ESD. Considering

the water supply target is more accessible to satisfy than the other two, especially in a wet year when only two targets need to be traded off. In comparison, the trade-offs among the three objectives can be more complex in a dry year.

4.2 Decision on operation schemes

The PDM proposed in Section 2 was applied to quantify the three objectives' trade-offs and decide the appropriate operation schemes. All non-inferior solutions were classified according to Equation (13), and the corresponding results are marked in Figures 7 and 8. The RR and N-PLSR of each solution were calculated in turn, and the sub-solution sets were filtered according to the principle of non-dominated sorting, as shown in Figure 11 below. Comparing Figures 7-9 reveals that the number of sub-set solutions has been significantly reduced compared to the original solution set, which greatly reduces the difficulty of decision-making.

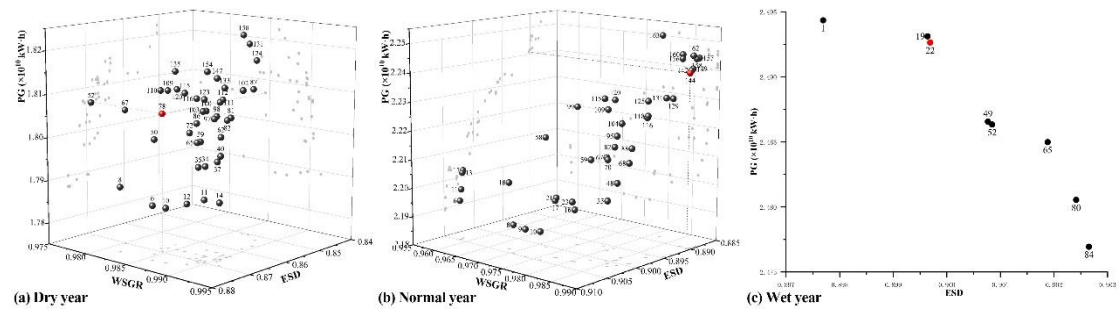


Figure 11 The sub-solution sets filtered by PDM, in which the red points represent the selected decision scheme

The PD to each target and the total PED of all solutions in the subsets were calculated according to Equation (20) ~ (21) and Equation (8) ~ (10), respectively, as shown in Table A1-A3 in the Appendix. Suppose the decision-maker prefers the benefits of the three objectives to be evenly distributed. In that case, the solution with the greatest PED (value of E in table A1-A3) will be chosen as the final decision scheme. Otherwise, if the decision maker has a stronger preference for any specific target, the solution with a relatively more minor PED (value of E) and a more extensive PD to this target (value of ω_1 or ω_2 or ω_3) will be chosen as the decision scheme. The overall process is intuitive and easy to operate.

As an example, the decision-maker has no particular preference for any target. The

schemes 78, 144 and 22 in Table A1-A3 can be selected as the operation schemes for dry, normal and wet years, respectively. The benefits obtained with the chosen schemes are shown in Table 4, and the corresponding reservoirs' water level processes are shown in Figure 12.

Table 4 Benefits by the objective of example decision schemes

	PG ($\times 10^{10}$ kW·h)	WSGR (%)	ESD (%)
Dry year	1.807	98.45	86.95
Normal year	2.241	98.95	89.03
Wet year	2.493	100.00	89.97

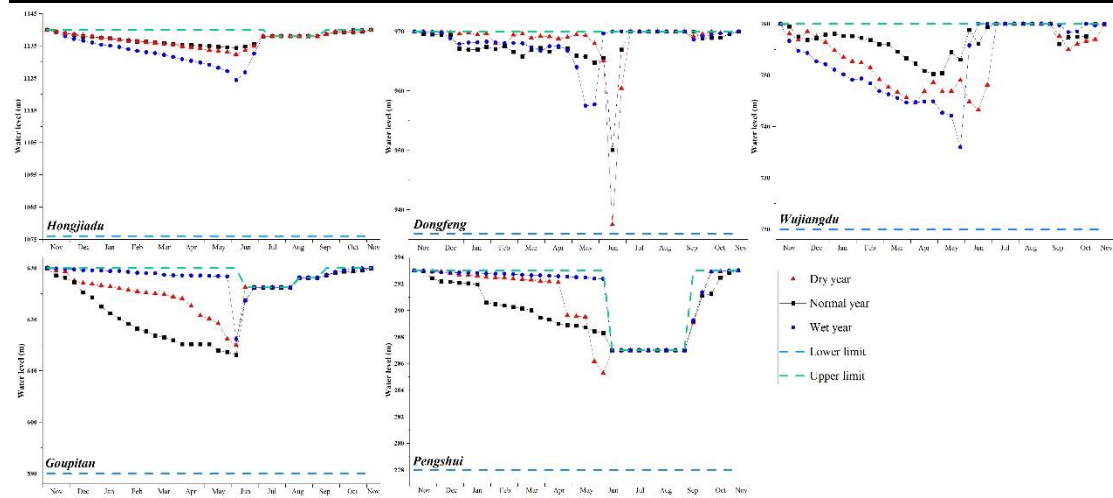


Figure 12 Water level processes for the example decision schemes

As a result, by optimizing the operation of the five reservoirs through the proposed PDM in this paper, the natural runoff can be fully used, and the comprehensive benefits can be enhanced considerably. The specific performance is shown as rationally increasing discharge during the non-flood season and utilizing the inflow during the flood season to replenish the water storage for the continuous profit-making function after the end of the flood season.

4.3 Discussion with existing technology

As mentioned earlier, many technologies are available for MCD in reservoir operation, and the application of PDM shows unique advantages.

As shown in Figure 11, PDM can effectively shrink the solution set and reduce the decision difficulty. The ϵ -dominance-based technique (Kollat and Reed, 2007) and the Competitiveness Index method (Wang et al., 2022) have made fruitful attempts on the practical limiting solution set. The difference is that the ϵ -dominance-based technique

improves the MOO process for the evolutionary algorithm (based on NSGA-II) using the ε -dominance strategy to improve the algorithm's efficiency without involving decision-making. In comparison, the Competitiveness Index method screens Pareto solutions based on the competitive efficiency among objectives. These methods limit the non-inferior solutions to a smaller size than the PDM method. Still, they can only retain a few solutions with the most conflicting benefits and will likely ignore some win-win options.

Many existing studies on the MCD process are inspired by the same economic idea of diminishing marginal utility as PDM, such as the method of finding the "knee area points" of the Pareto frontier (Li et al., 2021) and quantifying individual linkage slope (X. Wu et al., 2022). These methods are fruitful and have a solid mathematical theoretical basis. In fact, the shrunk solution set of the PDM is likely to contain the knee point solutions obtained by the above methods. The difference is that these approaches are dedicated to providing a monotonous option to the decision-maker, weakening their subjective initiative. However, actual reservoir operation activities often require considering different external conditions, and a monotonous theoretical optimal scheme cannot meet the practical needs. The PDM takes a step forward relative to these methods. By drawing on the idea of the Gini coefficient, two indicators, PD and PED, are proposed to quantify the degree of decision-maker's bias toward specific goals at different solutions and provide an intuitive reference for decision makers' subjective trade-offs. In addition, the simplicity of practical engineering operation is also an advantage of the PDM over other methods.

Overall, the most significant advantage of the PDM over existing technologies is that it can provide precise and reliable objective support for decision-maker's subjective preferences, which is more in line with the significance of "trade-off" in engineering practice. Finally, the above case study is a deterministic simulation operation using runoffs of three historical years. Besides, the PDM can also be applied to real-time operation through the loop of "hydrological forecast-optimization-decision making-reservoir status update".

5. Conclusion

Aiming at the trade-offs among objectives in MCD, this paper proposed the concepts of RR, PLSR, and PED and derived the PDM in the bi-objective and tri-objective scenarios. The PDM is based on the geometric relationship among Pareto solutions and uses universally acknowledged ideas of economics for reference. The method tries to provide a solid support for decision-maker's subjective preferences in a clear, quantitative, and objective manner and can achieve the unification of subjectivity and objectivity.

Applying the PDM to the cascade reservoirs in Wujiang River Basin, a multi-objective operation model with power generation, water supply, and ecological protection was developed and solved, and the results show that:

(1) Under different hydrological conditions, there are competitive relationships of different degrees among the various objectives of the cascade reservoirs in Wujiang River Basin, with the most substantial competition lying between the two benefits of PG and ESD, and the intensity of the competition ascends with the increase of natural inflow.

(2) Natural inflow has a significant influence on the benefit of each target at large favourably, particularly on power generation. Moreover, the positive effects of inflow can be more fully extended through reliable trade-offs for the benefit of environmental protection in wet years and water supply in normal years.

(3) The PDM can effectively shrink the Pareto solution set and reduce the difficulty of decision-making. The PD and PED can quantify the complex internal feedback relationship among different goals and assist decision-makers in making trade-offs on the interests of multiple subjects.

(4) The PDM is based entirely on the Pareto set itself, which requires no additional data, making it simple to utilize, and can be extended into solving other MODPs.

Several improvements can be incorporated into our proposed method. First, when facing four-, five-, or even higher-dimensional objectives problem, how to further promote the PDM need more derivation. In addition, for different river sections in the

upper, middle and lower reaches of the cascade reservoir group system, decision makers' preferences tend to change at different stages in the full cycle of reservoir operation. How to adapt to the spatial and temporal variability of decision makers' preferences is also an issue worthy of continued further study.

Reference:

- Alhazaymeh, K., Hassan, N., 2015. Vague soft set relations and functions. *Journal of Intelligent & Fuzzy Systems* 28, 1205–1212. <https://doi.org/10.3233/IFS-141403>
- Baghapour, M.A., Shooshtarian, M.R., Zarghami, M., 2020. Process Mining Approach of a New Water Quality Index for Long-Term Assessment under Uncertainty Using Consensus-Based Fuzzy Decision Support System. *Water Resour Manag* 34, 1155–1172. <https://doi.org/10.1007/s11269-020-02489-5>
- Bai, T., Chang, J., Chang, F.-J., Huang, Q., Wang, Y., Chen, G., 2015. Synergistic gains from the multi-objective optimal operation of cascade reservoirs in the Upper Yellow River basin. *J Hydrol* 523, 758–767. <https://doi.org/10.1016/j.jhydrol.2015.02.007>
- Brewer, P., Venaik, S., 2010. GLOBE practices and values: A case of diminishing marginal utility? *J Int Bus Stud* 41, 1316–1324. <https://doi.org/10/b3jkv7>
- Ceriani, L., Verme, P., 2012. The origins of the Gini index: extracts from *Variabilità e Mutabilità* (1912) by Corrado Gini. *J Econ Inequal* 10, 421–443. <https://doi.org/10/cv8wdh>
- Coello Coello, C.A., Van Veldhuizen, D.A., Lamont, G.B., 2002. Evolutionary Algorithm MOP Approaches, in: Coello Coello, C.A., Van Veldhuizen, D.A., Lamont, G.B. (Eds.), *Evolutionary Algorithms for Solving Multi-Objective Problems*. Springer US, Boston, MA, pp. 59–99. https://doi.org/10.1007/978-1-4757-5184-0_2
- Cohon, J.L., 1978. *Multiobjective Programming and Planning*. Academic Press, Inc., New York-London.
- Cruz Courtois, O.A. de la, Arganis Juárez, M.L., Guichard Romero, D., 2021. Simulated Optimal Operation Policies of a Reservoir System Obtained with Continuous Functions Using Synthetic Inflows. *Water Resour Manag* 35, 2249–2263. <https://doi.org/10.1007/s11269-021-02841-3>
- Fu, G., Kapelan, Z., Kasprzyk, J.R., Reed, P., 2013. Optimal Design of Water Distribution Systems Using Many-Objective Visual Analytics. *J Water Res Plan Man* 139, 624–633. [https://doi.org/10.1061/\(ASCE\)WR.1943-5452.0000311](https://doi.org/10.1061/(ASCE)WR.1943-5452.0000311)
- Garg, H., Kumar, K., 2018. An advanced study on the similarity measures of intuitionistic fuzzy sets based on the set pair analysis theory and their application in decision making. *Soft Comput* 22, 4959–4970. <https://doi.org/10.1007/s00500-018-3202-1>
- Hurford, A.P., Huskova, I., Harou, J.J., 2014. Using many-objective trade-off analysis to help dams promote economic development, protect the poor and enhance ecological health. *Environ Sci Policy* 38, 72–86. <https://doi.org/10.1016/j.envsci.2013.10.003>
- Kim, T., Heo, J.-H., Jeong, C.-S., 2006. Multi-reservoir system optimization in the Han River basin using multi-objective genetic algorithms. *Hydrol Process* 20, 2057–2075. <https://doi.org/10.1002/hyp.6047>
- Kollat, J.B., Reed, P.M., 2007. A computational scaling analysis of multiobjective evolutionary

- algorithms in long-term groundwater monitoring applications. *Advances in Water Resources* 30, 408–419. <https://doi.org/10/dxhhgg>
- Labadie, J.W., 2004. Optimal Operation of Multi-reservoir Systems: State-of-the-Art Review. *J Water Res Plan Man* 130, 93–111. [https://doi.org/10.1061/\(ASCE\)0733-9496\(2004\)130:2\(93\)](https://doi.org/10.1061/(ASCE)0733-9496(2004)130:2(93))
- Lei, G.-J., Wang, W.-C., Yin, J.-X., Wang, H., Xu, D.-M., Tian, J., 2019. Improved fuzzy weighted optimum curve-fitting method for estimating the parameters of a Pearson Type-III distribution. *Hydrological Sciences Journal* 64, 2115–2128. <https://doi.org/10.1080/02626667.2019.1620950>
- Li, F.-F., Liu, C.-M., Wu, Z.-G., Qiu, J., 2020. Balancing Ecological Requirements and Power Generation in Reservoir Operation in Fish Spawning Seasons. *Journal of Water Resources Planning and Management* 146, 04020074. [https://doi.org/10.1061/\(asce\)wr.1943-5452.0001277](https://doi.org/10.1061/(asce)wr.1943-5452.0001277)
- Li, J., Zhang, W., Yeh, W.W.-G., 2021. A Proposed Multi-Objective, Multi-Stage Stochastic Programming With Recourse Model for Reservoir Management and Operation. *Water Resources Research* 57, e2020WR029200. <https://doi.org/10/gqjvt5>
- Li, Y., Liu, S., Xu, L., Chen, H., Wang, H., 2015. Decision target adjustment quality function deployment network with an uncertain multi-level programming model for a complex product. *J Grey Syst-Uk* 27, 132+.
- Liu, X., Chen, L., Zhu, Y., Singh, V.P., Qu, G., Guo, X., 2017. Multi-objective reservoir operation during flood season considering spillway optimization. *J Hydrol* 552, 554–563. <https://doi.org/10.1016/j.jhydrol.2017.06.044>
- Luo, D., Wang, X., 2012. The multi-attribute grey target decision method for attribute value within three-parameter interval grey number. *Appl Math Model* 36, 1957–1963. <https://doi.org/10.1016/j.apm.2011.07.074>
- Malekmohammadi, B., Zahraie, B., Kerachian, R., 2011. Ranking solutions of multi-objective reservoir operation optimization models using multi-criteria decision analysis. *Expert Syst Appl* 38, 7851–7863. <https://doi.org/10.1016/j.eswa.2010.12.119>
- Meng, F., Fu, G., Butler, D., 2016. Water quality permitting: From end-of-pipe to operational strategies. *Water Res* 101, 114–126. <https://doi.org/10.1016/j.watres.2016.05.078>
- Ngo, L.L., Madsen, H., Rosbjerg, D., 2007. Simulation and optimization modelling approach for operation of the Hoa Binh reservoir, Vietnam. *J Hydrol* 336, 269–281. <https://doi.org/10.1016/j.jhydrol.2007.01.003>
- Ni, X., Dong, Z., Xie, W., Jia, W., Duan, C., Yao, H., 2019. Research on the Multi-Objective Cooperative Competition Mechanism of Jinsha River Downstream Cascade Reservoirs during the Flood Season Based on Optimized NSGA-III. *Water-Sui* 11, 849. <https://doi.org/10.3390/w11040849>
- Raynal Villaseñor, J.A., 2021. Pearson Type III Distribution, in: Raynal Villaseñor, J.A. (Ed.), *Frequency Analyses of Natural Extreme Events: A Spreadsheets Approach*, Earth and Environmental Sciences Library. Springer International Publishing, Cham, pp. 139–165. https://doi.org/10.1007/978-3-030-86390-6_7
- Reed, P.M., Kollat, J.B., 2013. Visual analytics clarify the scalability and effectiveness of massively parallel many-objective optimization: A groundwater monitoring design example. *Adv Water Resour* 56, 1–13. <https://doi.org/10.1016/j.advwatres.2013.01.011>

- Ridha, H.M., Gomes, C., Hizam, H., Ahmadipour, M., Heidari, A.A., Chen, H., 2021. Multi-objective optimization and multi-criteria decision-making methods for optimal design of standalone photovoltaic system: A comprehensive review. *Renewable and Sustainable Energy Reviews* 135, 110202. <https://doi.org/10/gh5wrv>
- Saaty, T.L., 2003. Decision-making with the AHP: Why is the principal eigenvector necessary. *Eur J Oper Res* 145, 85–91. [https://doi.org/10.1016/S0377-2217\(02\)00227-8](https://doi.org/10.1016/S0377-2217(02)00227-8)
- Şahin, R., Liu, P., 2017. Correlation coefficient of single-valued neutrosophic hesitant fuzzy sets and its applications in decision making. *Neural Comput & Applic* 28, 1387–1395. <https://doi.org/10.1007/s00521-015-2163-x>
- Schindele, S., Trommsdorff, M., Schlaak, A., Obergfell, T., Bopp, G., Reise, C., Braun, C., Weselek, A., Bauerle, A., Högy, P., Goetzberger, A., Weber, E., 2020. Implementation of agrophotovoltaics: Techno-economic analysis of the price-performance ratio and its policy implications. *Applied Energy* 265, 114737. <https://doi.org/10/gh3cj8>
- Smith, R., Kasprzyk, J., Rajagopalan, B., 2019. Using multivariate regression trees and multiobjective trade-off sets to reveal fundamental insights about water resources systems. *Environmental Modelling & Software* 120, 104498. <https://doi.org/10.1016/j.envsoft.2019.104498>
- Tang, R., Ding, W., Ye, L., Wang, Y., Zhou, H., 2019. Trade-off Analysis Index for Many-Objective Reservoir Optimization. *Water Resour Manag* 33, 4637–4651. <https://doi.org/10.1007/s11269-019-02363-z>
- Tzeng, G.-H., Huang, J.-J., 2011. *Multiple Attribute Decision Making: Methods and Applications*. CRC Press.
- Wang, H., Lei, X., Guo, X., Jiang, Y., Zhao, T., Wang, X., Liao, W., 2016. Multi-Reservoir System Operation Theory and Practice, in: Wang, L.K., Yang, C.T., Wang, M.-H.S. (Eds.), *Advances in Water Resources Management, Handbook of Environmental Engineering*. Springer International Publishing, Cham, pp. 1–110. https://doi.org/10.1007/978-3-319-22924-9_1
- Wang, H.-R., Li, F.-F., Wang, G.-Q., Qiu, J., 2022. Shrinking Pareto Fronts to Guide Reservoir Operations by Quantifying Competition Among Multiple Objectives. *Water Resour Res* 58, e2021WR029702. <https://doi.org/10.1029/2021WR029702>
- Wang, X., Dong, Z., Ai, X., Dong, X., Li, Y., 2020. Multi-objective model and decision-making method for coordinating the ecological benefits of the Three Gorges Reservoir. *J Clean Prod* 270, 122066. <https://doi.org/10.1016/j.jclepro.2020.122066>
- Wei, Y., Dong, Z., 2021. Application of a Novel Jaya Algorithm Based on Chaotic Sequence and Opposition-based Learning in the Multi-objective Optimal Operation of Cascade Hydropower Stations System. *Water Resour Manag* 35, 1397–1413. <https://doi.org/10.1007/s11269-020-02731-0>
- Wu, C., Wang, Y., Ji, J., Liu, P., Li, L., Feng, M., 2022. Deriving reservoir operating rules considering ecological demands of multiple stations. *Proceedings of the Institution of Civil Engineers - Water Management* 1–14. <https://doi.org/10.1680/jwama.21.00009>
- Wu, L., Bai, T., Huang, Q., 2020. Trade-off analysis between economic and ecological benefits of the inter basin water transfer project under changing environment and its operation rules. *J Clean Prod* 248, 119294. <https://doi.org/10.1016/j.jclepro.2019.119294>
- Wu, X., Yu, L., Wu, S., Jia, B., Dai, J., Zhang, Y., Yang, Q., Zhou, Z., 2022. Trade-Offs in the Water-

- Energy-Ecosystem Nexus for Cascade Hydropower Systems: A Case Study of the Yalong River, China. *Front Env Sci-Switz* 10. <https://doi.org/10.3389/fenvs.2022.857340>
- Yang, G., Guo, S., Li, L., Hong, X., Wang, L., 2016. Multi-Objective Operating Rules for Danjiangkou Reservoir Under Climate Change. *Water Resour Manag* 30, 1183–1202. <https://doi.org/10.1007/s11269-015-1220-7>
- Yang, T., Liu, X., Wang, L., Bai, P., Li, J., 2020. Simulating Hydropower Discharge using Multiple Decision Tree Methods and a Dynamical Model Merging Technique. *J Water Res Plan Man* 146, 04019072. [https://doi.org/10.1061/\(ASCE\)WR.1943-5452.0001146](https://doi.org/10.1061/(ASCE)WR.1943-5452.0001146)
- Zhang, S., Chang, T., Wang, Y., 2018. Spatial and Seasonal Precipitation Variability in Eastern Fujian Based on Automatic Station Observation Data. *Sensors and Materials* 525. <https://doi.org/10.18494/SAM.2018.1822>

Data Availability Statements

The data that support the findings of this study are available from the corresponding author upon reasonable request.

Acknowledgement:

This research was funded by the National Key Research & Development Project of China, grant number 2016YFC0402209, and the China Scholarship Council. We also would like to thank Mr. Zhuolin He of Water Resources Bureau of Qiannan Prefecture, Guizhou Province, China for his assistance in providing some runoff data and reservoirs' parameters.

Appendix

Table A1 The Pareto subset and its corresponding PD and PED in typical dry year

No.	ω_1	ω_2	ω_3	E	No.	ω_1	ω_2	ω_3	E	No.	ω_1	ω_2	ω_3	E
6	0.2669	0.0403	0.6927	0.2014	65	0.0001	0.3996	0.6003	0.0005	110	0.0157	0.0252	0.9591	0.0102
8	0.3655	0.0050	0.6296	0.0310	67	0.9431	0.0193	0.0376	0.0185	111	0.0206	0.9363	0.0431	0.0225
10	0.1444	0.0046	0.8510	0.0153	72	0.3125	0.6249	0.0626	0.3299	112	0.0206	0.9363	0.0431	0.0225
11	0.2369	0.0058	0.7572	0.0283	78	0.6752	0.2060	0.1188	0.4460	115	0.6161	0.0141	0.3698	0.0868
12	0.9517	0.0191	0.0292	0.0143	81	0.0186	0.8910	0.0904	0.0404	116	0.0433	0.0130	0.9438	0.0143
14	0.3122	0.0873	0.6005	0.4418	82	0.2127	0.7107	0.0766	0.3125	120	0.9202	0.0138	0.0660	0.0226
34	0.0039	0.0961	0.9000	0.0090	86	0.0900	0.7798	0.1302	0.2467	123	0.0433	0.0016	0.9551	0.0018
35	0.9924	0.0064	0.0012	0.0002	87	0.0068	0.4966	0.4966	0.0453	124	0.1096	0.8499	0.0405	0.1019
37	0.0239	0.9650	0.0112	0.0070	97	0.0530	0.8329	0.1141	0.1359	131	0.9680	0.0216	0.0105	0.0059
40	0.0239	0.9649	0.0112	0.0070	98	0.0530	0.8329	0.1140	0.1360	133	0.0168	0.8827	0.1005	0.0402
50	0.6241	0.0044	0.3716	0.0274	100	0.0011	0.1015	0.8973	0.0028	135	0.0035	0.1172	0.8793	0.0096
52	0.5964	0.0043	0.3993	0.0277	102	0.0048	0.9915	0.0037	0.0005	147	0.0103	0.7221	0.2676	0.0537
59	0.0001	0.3996	0.6003	0.0005	103	0.0328	0.0974	0.8698	0.0751	150	0.9827	0.0134	0.0039	0.0014
62	0.1761	0.8110	0.0130	0.0499	109	0.0157	0.0252	0.9591	0.0102	154	0.9368	0.0227	0.0405	0.0232

Table A2 The Pareto subset and its corresponding PD and PED in typical normal year

No.	ω_1	ω_2	ω_3	E	No.	ω_1	ω_2	ω_3	E	No.	ω_1	ω_2	ω_3	E
6	0.96213	0.01333	0.02453	0.00850	58	0.94418	0.00001	0.05581	0.00001	120	0.05807	5×10^{-7}	0.94193	1×10^{-6}
8	0.54551	0.00001	0.45448	0.00003	59	0.05297	0.00001	0.94702	0.00001	125	0.10901	0.00004	0.89095	0.00010
9	0.54544	0.00001	0.45455	0.00003	67	0.00413	4×10^{-6}	0.99586	5×10^{-7}	129	0.00877	0.82392	0.16730	0.03265
10	0.25725	0.00002	0.74273	0.00010	68	0.91863	0.00085	0.08051	0.00170	131	0.00876	0.82397	0.16726	0.03261
11	0.96218	0.01333	0.02448	0.00848	70	0.00413	4×10^{-6}	0.99587	5×10^{-7}	144	0.38688	0.42671	0.18642	0.83090

13	0.36986	0.12157	0.50857	0.61742	82	0.99800	0.00003	0.00197	2×10^{-6}	147	0.15851	0.30439	0.53710	0.69970
15	0.56348	0.37413	0.06240	0.35515	88	0.01768	0.00002	0.98229	0.00001	149	0.15858	0.30440	0.53701	0.69993
16	0.95866	0.00073	0.04061	0.00077	95	0.03377	0.00142	0.96480	0.00125	156	0.95782	0.00240	0.03979	0.00247
17	0.93833	0.00071	0.06096	0.00110	99	0.18734	0.00001	0.81264	0.00005	157	0.01414	0.01863	0.96723	0.00688
18	0.89207	1×10^{-6}	0.10793	2×10^{-6}	104	0.93636	0.00005	0.06359	0.00007	158	0.01413	0.01863	0.96724	0.00687
21	0.93836	0.00071	0.06093	0.00110	109	0.66511	0.00000	0.33488	0.00002	160	0.95784	0.00240	0.03976	0.00246
23	0.52625	0.00011	0.47364	0.00075	115	0.05806	5×10^{-7}	0.94194	1×10^{-6}	162	0.00068	0.99839	0.00092	0.00002
35	0.84024	0.00307	0.15669	0.01090	116	0.99188	0.00005	0.00807	0.00001	163	0.22060	1×10^{-6}	0.77940	4×10^{-6}
48	0.01957	0.00002	0.98041	0.00001	118	0.99189	0.00005	0.00806	0.00001					

Table A3 The Pareto subset and its corresponding PD and PED in typical wet year

No.	ω_1	ω_2	E												
1	0.9991	0.0009	0.0038	22	0.5168	0.4832	0.9989	52	0.9739	0.0261	0.1017	80	0.0683	0.9317	0.2544
19	0.9999	0.0001	0.0004	49	0.4229	0.5771	0.9762	65	0.0006	0.9994	0.0022	84	0.0015	0.9985	0.0061